Biochimica et Biophysica Acta 1828 (2013) 1230–1240

Contents lists available at SciVerse ScienceDirect

Biochimica et Biophysica Acta

journal homepage: www.elsevier.com/locate/bbamem

Glutamate efflux mediated by *Corynebacterium glutamicum* MscCG, *Escherichia coli* MscS, and their derivatives

Michael Becker [a], Kirsten Börngen [a], Takeshi Nomura [b], Andrew R. Battle [b,d], Kay Marin [a], Boris Martinac [b,c], Reinhard Krämer [a,*]

[a] Institute of Biochemistry, University of Cologne, Zülpicher Str. 47, 50674 Köln, Germany
[b] Victor Chang Cardiac Research Institute, Darlinghurst, Sydney, NSW 2010, Australia
[c] St. Vincent's Clinical School, The University of New South Wales, Sydney, NSW 2052, Australia
[d] School of Pharmacy, Griffith University, Parklands, QLD 4222, Australia

ARTICLE INFO

Article history:
Received 13 September 2012
Received in revised form 13 December 2012
Accepted 1 January 2013
Available online 10 January 2013

Keywords:
Corynebacterium
Glutamate excretion
Mechanosensitive channel
Efflux
MscS
MscCG

ABSTRACT

Corynebacterium glutamicum is used in microbial biotechnology for the production of amino acids, in particular glutamate. The mechanism of glutamate excretion, however, is not yet fully understood. Recently, evidence was provided that the *NCgl1221* gene product from *C. glutamicum ATCC 13869*, a MscS-type mechanosensitive efflux channel, is responsible for glutamate efflux [1]. The major difference of NCgl1221 and the homologous protein MscCG of *C. glutamicum* ATCC 13032 from *Escherichia coli* MscS and most other MscS-type proteins is the presence of an additional, 247 amino acid long C-terminal domain. By topology analysis, we show that this domain in MscCG carries a transmembrane segment. We have generated selected C-terminal truncations of MscCG, gain-of-function and loss-of-function constructs of both *E. coli* MscS and *C. glutamicum* MscCG, as well as fusion constructs of the two proteins. These mutant proteins were investigated for mechanosensitive efflux, MS channel activity, glutamate excretion and their impact on membrane potential. We provide evidence that the channel domain of MscCG mediates glutamate efflux in response to penicillin treatment, and that the *E. coli* MscS channel is to some extent able to function in a similar manner. We further show that the C-terminal domain of MscCG has a significant impact for function and/or regulation of MscCG. Significantly, a positive effect on glutamate efflux of the C-terminal extension of MscCG from *C. glutamicum* was also observed when fused to the *E. coli* MscS channel.

1. Introduction

Specific transport systems responsible for the excretion of various amino acids by *Corynebacterium glutamicum* have been characterized and identified in the last two decades [2–4], but a system responsible for the well-known glutamate excretion activity of *C. glutamicum* was missing for a long time. This situation changed upon the experimental correlation of glutamate efflux in *C. glutamicum* with the presence of a protein related to MscS from *Escherichia coli* [1]. This pioneering work provided evidence for the NCgl1221 gene product, a homolog of MscCG described here, being responsible for glutamate efflux in *C. glutamicum*. A basic problem, however, related with strategies to identify transport systems by inactivation and complementation, was not solved. It is inherently difficult to decide between the function of a candidate protein as a transporter or as a regulator of another, possibly not yet identified transport system. A well-known example of this kind of scenario is the glucose-6-phosphate transport system UhpT and the structurally closely related regulator UhpC in *E. coli* [5].

The gene product NCgl1221, studied by Nakamura et al. [1] and others [6,7], as well as MscCG [8,9], are members of the protein family of MscS-type mechanosensitive channels with respect to their N-terminal part which represents the channel domain. In addition, and in difference to *E. coli* MscS-type channels, NCgl1221 and MscCG, respectively, carry a long C-terminal extension of so far unknown function. The basic physiological function of mechanosensitive channels is to open in cases of emergency, thus avoiding the adverse effects of massive water influx in response to hypo-osmotic stress by causing fast release of small internal solutes [10]. By studying MscCG of *C. glutamicum*, we recently showed that this type of protein, besides being a typical mechanosensitive channel [9], is required, in addition, for fine-tuning the osmotic balance also under hyperosmotic conditions [8].

In this study we were interested in two important aspects of the MscCG protein, first, to convincingly assign the channel function of MscCG to glutamate efflux and second, to learn more about a putative specific function of the unique C-terminal extension. The latter seems to be an individual feature of MscCG and closely related proteins. For

* Corresponding author. Tel.: +49 221 6461; fax: +49 221 5091.
E-mail address: r.kraemer@uni-koeln.de (R. Krämer).

0005-2736/$ – see front matter © 2013 Elsevier B.V. All rights reserved.
http://dx.doi.org/10.1016/j.bbamem.2013.01.001

this purpose we constructed a repertoire of tools including truncated versions of MscCG altered in the size of their C-terminal domain, both gain of function and loss of function mutants of MscCG and of *E. coli* MscS heterologously expressed in *C. glutamicum*, as well as appropriate fusion constructs between MscCG and MscS. Using these tools in biochemical, physiological and electrophysiological experiments, we provide clear evidence for glutamate flux under conditions of triggered glutamate excretion being mediated by the channel part of MscCG, on the one hand, and for the C-terminal domain of MscCG being of significant impact for function and/or regulation of MscCG, on the other.

2. Materials and methods

2.1. Strains, media and growth conditions

E. coli strains DH5αmcr [11] and *C. glutamicum* wild-type strain ATCC13032 and its derivatives (this work) were used (Table S1 in the supporting material). *E. coli* was grown at 37 °C in Luria–Bertani medium, *C. glutamicum* at 30 °C in brain heart infusion (BHI, Difco, Detroit, USA) or in CgXII medium (pH 7.0) containing per l: 20 g $(NH_4)_2SO_4$, 5 g urea, 1 g KH_2PO_4, 1.6 g K_2HPO_4, 42 g MOPS, 2.9 g NaCl, 4% glucose, 0.25 g $MgSO_4$, 0.01 g $CaCl_2$, 0.2 mg biotin, 30 mg protocatechuate, 1 ml of a solution of trace elements [12]. For growth under different osmolalities MM1 medium (pH 7.0) was used containing per l: 5 g $(NH_4)_2SO_4$, 5 g urea, 2 g KH_2PO_4, 2 g K_2HPO_4, 3 g NaCl, 4% glucose, 0.25 g $MgSO_4$, 0.01 g $CaCl_2$, 0.2 mg biotin, 30 mg protocatechuate, 1 ml of a solution of trace elements and 0, 200 or 400 mM NaCl. Antibiotics were added in concentrations of 100 μg/ml for *E. coli* and 25 μg/ml for *C. glutamicum*.

2.2. Strain construction

Deletion of the *mscCG* gene (*NCgl1221*) was performed by cross over PCR [13] and double homologous recombination using the suicide vector pK19mobsacB_*ΔmscCG* [8], and was verified by PCR analysis. For complementation the *mscCG* gene was amplified by PCR using *C. glutamicum* ATCC 13032 chromosomal DNA as template. The amplified fragment was cleaved by BamHI and SalI and ligated into BamHI/SalI-cleaved pEKex2, resulting in pEKex2_*mscCG* or pEKex2_*mscCG*-His, respectively. Truncations of *mscCG* were subcloned from pET29b into the *E. coli–C. glutamicum* shuttle vector pEKex2. For this purpose, fragments were cleaved by B1pI and XbaI. Upon refill of 3'-end overhangs, fragments were ligated into pEKex2 cleaved by Ecl136II. Similar to this procedure *E. coli mscS* was amplified via PCR using MG1655 chromosomal DNA as template. The amplified fragment was cleaved by BamHI and NotI and ligated into BamHI/NotI-cleaved pEKex2, resulting in pEKex2_*mscS*-His. The fusion of the *E. coli mscS* gene with the C-terminal domain of *C. glutamicum mscCG* was accomplished by PCR using the corresponding template DNAs as described previously [14]. The amplified fragments were cleaved by BamHI and NotI and ligated into the BamHI/NotI-cleaved pEKex2, resulting in pEKex2_*mscS_C_MscCG-his*. These plasmids were introduced into ATCC 13032 Δ*mscCG* by electroporation. All strains and plasmids are listed in Table S1.

For topology analysis *MscCG* gene variants encoding the full length protein as well as different truncated forms were fused to an alkaline phosphatase-β-galactosidase reporter cassette [15] and transformed in *E. coli* BL21 (DE3) cells using the *E. coli C. glutamicum* shuttle vector pMS3. With the resulting strains β-galactosidase as well as alkaline phosphatase activity assays were performed.

To obtain GOF mutants, the 3D structure of MscCG was modeled by the *SWISS-MODEL workspace* [16] based on the known structure of MscS from *E. coli* [17]. As likely candidates, A106 and L109 at highly similar locations (both residues are identical in the two proteins) compared to MscS were identified. Both amino acids are located in the 3rd transmembrane domain, which is highly conserved in proteins of the MscS-family building the pore of the MscS-type channel. Small polar substitutions (L111S and L115S) in the gate-forming TM3 of MscS resulted in a loss-of-function (LOF) phenotype after osmotic shocks [18]. In a first step, we aligned the amino acid sequences of the closed form of MscS lacking the first N-terminal 26 amino using "Jalview" and "T-COFFEE" [19,20]. Finally, modeling with Modeller [21] revealed 20 putative structures of MscCG. The most probable model based on the consistency of coordinates was used for determining equivalent amino acids for a LOF mutation in MscCG. Site-directed mutagenesis for generating GOF and LOF mutations in pEKex2_*mscS_C_mscCG-his* and pEKex2_*mscCG*-his was performed using the Stratagene Quickchange Site-Directed Mutagenesis protocol to introduce single amino acid replacements by using mutagenic primer pairs. Subsequent to the PCR, the methylated initial template DNA was digested by addition of 1 μl DpnI and the residual DNA was transformed into *E. coli* DH5α competent cells.

2.3. Preparation of giant spheroplasts

E. coli strain MJF612 lacking MscL, MscS, MscK, and MscM expressing the plasmid encoded *mscCG* of *C. glutamicum* was used for preparation of giant spheroplasts [22]. Since the MJF612 strain harbors kanamycin, apramycin and chloramphenicol resistance a new vector was constructed. The pQE60 vector (ampicillin resistance) was fused to the *lacI* gene normally encoded on a second plasmid. The *mscCG* gene was amplified via PCR using ATCC 13032 chromosomal DNA as template. The amplified fragment and the fragments of the truncated *mscCG* constructs were cleaved by NcoI and BamHI and ligated into NcoI/BamHI-cleaved pQE60-lacI. The procedure used for the preparation of giant spheroplasts from the new *E. coli* strain expressing MscCG protein was as described previously [8]. *E. coli* MJF465 [23] lacking MscS, MscL, and MscK was used for the preparation of giant spheroplasts when expressing MscS and MscS-C-MscCG.

2.4. Electrical recording

Single-channel analysis was performed on giant *E. coli* spheroplasts [24]. Spheroplasts (1.5–3 μl) were placed in a bath containing, unless otherwise stated, 250 mM KCl, 90 mM $MgCl_2$, and 5 mM HEPES (pH 7.2). Borosilicate glass pipettes (Drummond Scientific Co., Broomall, PA) were pulled using a Flaming/Brown pipette puller (P-87, Sutter Instrument Co., Novato, CA) to a diameter that corresponded to a pipette resistance between 3.0 and 6.0 MΩ. The pipettes were filled with 200 mM KCl, 90 mM $MgCl_2$, and 5 mM HEPES (pH 7.2). All recordings were made at room temperature (19–23 °C) by applying negative pressure (suction) recorded in mm Hg to patch pipettes by using a syringe and were monitored using a piezoelectric pressure transducer (Omega Engineering, Stamford, USA). Ion currents arising from activation of the proteins using suction were recorded using an Axopatch 1D patch-clamp amplifier (Axon Instruments), filtered at 2 kHz and digitized at 5 kHz. Single channel analysis was done using pCLAMP10 software (Axon Instruments). Furthermore, MscCG activity was compared to that of MscS by determining its threshold of activation relative to the MscL activation threshold, which has served as a standard [25].

2.5. Enzyme assays

For alkaline phosphatase and β-galactosidase activity determinations, LB overnight cultures of *E. coli* BL21 cells harboring the pMS3 plasmid with different *mscCG* truncations were diluted to an OD_{600} of 1. Cells were permeabilized by addition of 70 μl 0.1% sodium deoxycholate and 70 μl toluene. After incubation for 30 min at 37 °C, 1 ml assay buffer was added (10 mM Tris, 10 mM $MgSO_4$, pH 8 for alkaline phosphatase and 37 mM NaH_2PO_4, 63 mM Na_2HPO_4, 1 mM $MgSO_4$, 0.2 mM $MnSO_4$ for β-galactosidase). Alkaline phosphatase activity was assayed essentially as described by Brickman and Beckwith [26], except using an extinction coefficient of $\varepsilon_{405nm} = 1.85 \times 10^{-4}\ M^{-1}\ cm^{-1}$ with

5-bromo-4-chloro-3-indolyl phosphate disodium salt as a substrate, whereas β-galactosidase was assayed according to Miller [27] with nitrophenyl-b-galactoside using an extinction coefficient of $\varepsilon_{420nm} = 2.13 \times 10^{-4}\ M^{-1}\ cm^{-1}$.

2.6. Uptake and efflux of glycine betaine and glutamate

Synthesis of [^{14}C]-labeled glycine betaine was performed as described previously [28]. For measurement of betaine efflux in response to hypoosmotic stress, *C. glutamicum* strains were grown aerobically at 30 °C at 125 rpm overnight in BHI medium containing 500 mM NaCl. Cells were harvested by centrifugation and washed twice under hypo-osmotic conditions in 100 mM MES/Tris, pH 8.0, 4 °C, containing 5 mM Na_2HPO_4 and 5 mM K_2HPO_4. This hypo-osmotic washing step results in efflux of the majority of compatible solutes, which were taken up or synthesized during the growth period. Uptake of the labeled betaine was performed by incubating the cells at an OD_{600} of 4 for 80 min at 30 °C in a hyper-osmotic buffer (100 mM MES/Tris pH 8.0) containing 0.9 M NaCl, 30 mM glucose, 30 mM urea and 30 mM KCl. Shortly after transfer into the uptake buffer [^{14}C]-glycine betaine at a final concentration of 1 mM (25,000 cpm/ml) was added. After loading of the cells with labeled betaine, they were stored on ice until used. To measure the efflux, cells were centrifuged and resuspended in 100 mM MES/Tris pH 8.0, containing various concentrations of NaCl to obtain appropriate osmolalities. After 15 s 200 µl samples were withdrawn and cells were rapidly separated from the surrounding medium by silicone oil centrifugation (oil density of 1.09 kg/l for osmolalities > 1.2 osmol/kg and 1.03 kg/l for osmolalities <1.2 osmol/kg) and counted.

Glutamate excretion was induced during the exponential growth phase by the addition of 0.15% Tween 60 or 6 U/ml Penicillin G. For the biotin-limited conditions a 24 h pre-culture in CgXII minimal medium containing 0.5 µg/l biotin was necessary [29]. Concentrations of external glutamate were determined by HPLC analysis.

2.7. Determination of membrane potential

The membrane potential was determined as described earlier [30]. The membrane potential was calculated from the distribution of the permeant cation [^{14}C]-tetraphenylphosphonium bromide (5 µM final concentration, specific radioactivity 0.995 Ci/mol). Rapid separation of extra- and intracellular fluids was performed by using silicone oil centrifugation with perchloric acid in the bottom layer [31]. The obtained values of membrane potential were corrected for unspecific probe binding by addition of a mixture of 20 µM valinomycin and 5 µM nigericin.

2.8. Protein synthesis and Western blot analysis

To control the expression of *mscCG* mutants, cells were disrupted using a Ribolyser (Thermo Co.) three times at maximum speed of 6.5 for 45 s. After separation of cell debris membranes were isolated by centrifugation and resuspended in PBS buffer, pH 7.5. Protein concentration was measured by the Bradford technique [32]. Western blot analysis was performed as described [12] using antibodies raised against 6×His-tag (Qiagen, Hilden) and against MscCG (Eurogentech, Cologne). As secondary antibodies anti-mouse-(AP) and anti-rabbit-(AP) (Sigma) antibodies were used.

3. Results

3.1. The C-terminal domain of MscCG: truncation constructs and their phenotype

C. glutamicum MscCG consists of 533 amino acids, including an N-terminal part (286 residues, *NCgl1221* gene), which is similar to other MscS-type proteins present in a variety of bacteria, the best known being MscS of *E. coli*. These proteins have a size of up to 350 amino acids and do not contain sequences related to the 247 residues long C-terminal part of MscCG. Protein sequences similar to the C-terminal domain of MscCG are exclusively found in predicted MS channel proteins of other *Corynebacteriaceae* (Fig. S1). Even closely related Mycobacteria lack this C-terminal extension. The observed sequence similarity is most significant in a region predicted to represent a fourth transmembrane domain (topology analysis see below). We thus conclude that the C-terminal domain is a characteristic and exclusive feature of MscCG and its close relatives in the group of *Corynebacteriaceae*.

In a recently published study on the NCgl1221 gene product, an MscCG homolog in *C. glutamicum* ATCC 13869 [1], which is closely related to *C. glutamicum* ATCC 13032 used in this work, a number of glutamate excreting strains were found to harbor mutations in the C-terminal domain of the MscCG protein. Based on these results, and to study structure/function relations in MscCG, we generated strategically positioned truncations in the C-terminal domain. As a prerequisite for this strategy we analyzed the topology of MscCG, which has only been suggested based on computer prediction [1,33]. The N-terminal part of MscCG is similar to MscS from *E. coli*, thus an identical topology was assumed. Depending on the kind of computer program used, the presence or absence of an additional transmembrane segment in the C-terminal domain of MscCG is predicted [33]. By using *lacZ* and *phoA* fusions of *mscCG*, we determined the topology of MscCG, revealing the presence of a fourth transmembrane segment, in addition to the three conserved segments in the N-terminal part (Table 1), matching the previously proposed topology [1]. Based on this result, we constructed several truncation mutants, i.e. His-tagged truncations missing the C-terminal 110 (MscCG-Δ110-His), 141 (MscCG-Δ141-His), and 247 (MscCG-Δ247-His) amino acids, respectively (Fig. 1A). MscCG-Δ110-His misses the terminal hydrophilic part of the C-terminal domain exposed to the periplasm, whereas MscCG-Δ141, in addition, lacks the fourth transmembrane segment. At first, instead of MscCG-Δ141-His, we used the mutant MscCG-Δ132-His (Table 1), which might be more precisely lacking the transmembrane segment. In the biochemical experiments, however, the expression of this recombinant form was not efficient enough (not shown). MscCG-Δ247-His is truncated to exactly the size of MscS thus consisting of the channel part only.

All constructs were expressed in the *mscCG* deletion strain. Some of the constructs resulted in lack of growth at IPTG concentrations generally used for expression (0.1 to 1 mM), but we succeeded with addition of 25 µM IPTG only. The mutant strains were cultivated at different osmolalities of 0.45, 0.75, 0.93, 1.10, and 1.29 osmol/kg. Growth was slightly affected in the strains MscCG-Δ141-His and MscCG-Δ247-His (not shown), whereas strain MscCG-Δ110-His showed an increased lag phase, in particular at increased osmolality (Fig. 1B and C). Expression of all constructs was quantified (Fig. 1D). It has previously been documented that expression of plasmid-encoded wild type *mscCG* is low and that of the genomic copy is not detectable [8]. The *mscCG*-Δ141-His and *mscCG*-Δ247-His constructs were strongly expressed in

Table 1
Membrane topology of *C. glutamicum* MscCG analyzed by fusion constructs.

Construct	ß-gal/AP activity
MscCG	1.31 ± 0.59
MscCG-Δ110	1.17 ± 0.58
MscCG-Δ132	10.7 ± 3.3
MscCG-Δ247	14.7 ± 6.9

The indicated fusion constructs of ß-galactosidase and alkaline phosphatase were expressed in *E. coli* BL21 (DE3) and the respective enzyme activities were measured. Mean values and standard deviation of at least three experiments are given.

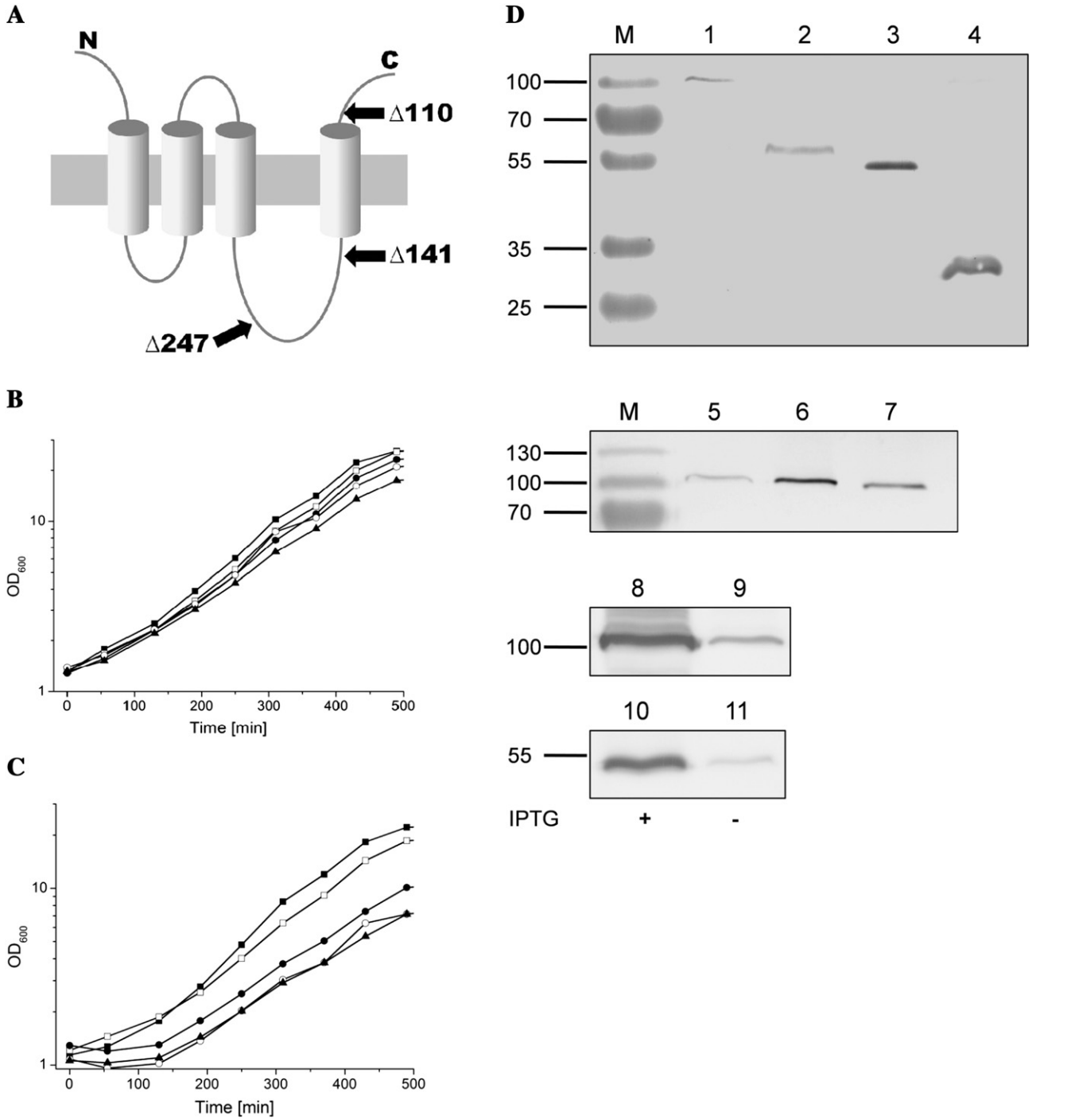

Fig. 1. Truncation constructs of MscCG and their properties. (A) Schematic representation of MscCG truncation constructs used in this work. (B) Growth of *C. glutamicum* wild type at different values of external osmolality (0.45 (solid squares), 0.75 (open squares), 0.93 (solid circles), 1.10 (open circles), and 1.29 osmol/kg (triangles)). The growth medium was supplemented with appropriate amounts of NaCl. (C) Growth of the *C. glutamicum* mscCG deletion strain expressing mscCG-Δ110-His, conditions and symbols as in (B). (D) Western blot analysis of mscCG and mscCG truncation constructs expressed in *C. glutamicum* ΔmscCG. His-tagged constructs of mscCG and its truncated versions were analyzed. 20 μg (MscCG-His, MscCGΔ141-His, MscCG_Q112L_V115S-His), 40 μg (MscCGΔ110-His, MscCGΔ247-His) and 10 μg (MscCG_A106V-His) of membrane extract were loaded to each gel, the blot was developed using anti-His antibody. The lanes are as follows: marker (M), MscCG-His, 25 μM IPTG (1, 5, 8), MscCGΔ110-His, 25 μM IPTG (2), MscCGΔ141-His, 25 μM IPTG (3, 10), MscCGΔ247-His, 50 μM IPTG (4), MscCG-Q112L/V115S-His (LOF), 25 μM IPTG (6), MscCG_A106V-His (GOF), 25 μM IPTG (7), MscCG-His, no IPTG (9), MscCG Δ141-His, no IPTG (11). In order to make the low level of MscCG proteins in lanes 9 and 11 detectable, the two gels with lanes 9 to 11 were developed much longer than the gels with lanes 1 to 7.

C. glutamicum, *mscCG*-Δ110-His expression was low. In spite of its low expression, *mscCG*-Δ110-His had a very strong influence on physiological properties and glutamate excretion (see below), thus proving its significance.

3.2. Solute flux in C. glutamicum harboring truncated versions of MscCG

The properties of MscCG as a mechanosensitive channel have been described previously in physiological and electrophysiological terms

[6–9]. We expressed various forms of *mscCG* in *C. glutamicum* grown at elevated osmolality, exposed the cells to a cycle of hypo- and hyperosmotic shocks for effective betaine loading, and finally tested for betaine efflux at decreasing osmolality as a functional measure of channel activity (Fig. 2A). Efflux in the *mscCG* complementation strain and the strains carrying the *mscCG*-Δ141-His and *mscCG*-Δ247-His constructs were identical, resp. similar to the wild type. In contrast, the strain harboring *mscCG*-Δ110-His deviated from the basic efflux pattern.

We also investigated the electrophysiological properties of the mutants. In patch-clamp experiments, the conductance was determined using I/V plots obtained in KCl/$MgCl_2$ containing buffers (Fig. 3 and Table 2). The experiments were carried out in the quadruple deletion strain *E. coli* MJF612, lacking MscL, MscS, MscK, and MscM, thus avoiding any interference by endogeneous mechanosensitive channels, in particular by those of similar conductance, e.g. MscM. We found rectifying behavior also for the truncation constructs, as previously described for the intact MscCG channel [8]. Notably, the conductance was more or less unchanged in all truncation constructs compared to the wild type. The results further indicate a similar lack of ion selectivity for anions and cations. Conductance of MscCG-Δ110-His could only be measured in the presence of 50 μM $GdCl_3$ because no appropriate seal was obtained in the absence of the channel blocker. In a control experiment we measured the conductance of the MscCG wild type protein upon addition of the same concentration of $GdCl_3$ and found, besides strong reduction of the number of channels, no significant change in electrical conductance (similar to Fig. 3A, data not shown).

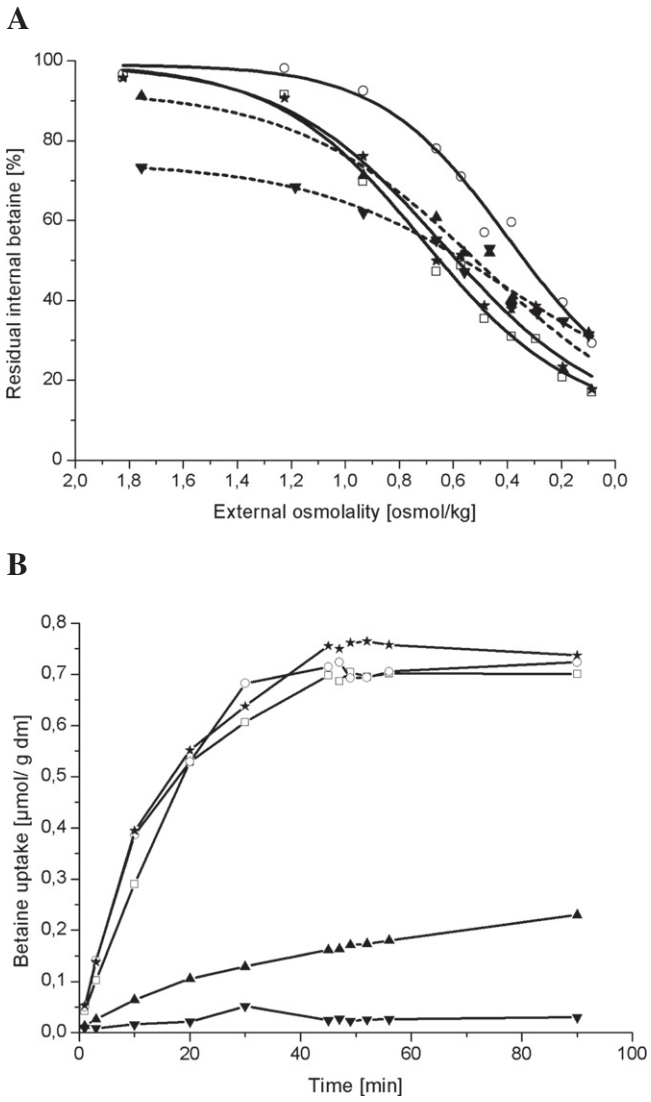

Fig. 2. Betaine uptake and efflux upon hypo-osmotic shock. (A) Betaine efflux was measured in cells after loading with labeled betaine and exposure to hypo-osmotic stress of different extent (see Materials and methods section). The strains used were as follows: wild type (open squares), *mscCG* deletion strain (open circles) expressing the following constructs: *mscCG* (stars), *mscCG*-Δ110-His (downward triangles, dashed line), *mscCG*-Δ247-His (upward triangles, dashed line). (B) Uptake of labeled betaine in the same strains, symbols as in (A). dm = dry mass.

For a functional comparison, relative values of betaine efflux had been plotted in Fig. 2A, which to some extent conceals the true situation. Analysis of betaine efflux requires the previous loading of cells with labeled betaine *via* the transporter BetP [34,35]. Since we observed a different effectiveness of loading in the strains tested, we analyzed the loading procedure in more detail (Fig. 2B). Wild type, deletion and complementation strains were identical in their behavior. A decreased loading was observed for strains harboring *mscCG*-Δ247-His and *mscCG*-Δ110-His, the latter being nearly fully impaired. This indicates that MscCG and its variants are responsible for this difference.

Three mechanistic explanations for this observation can be proposed: (i) recombinant forms of MscCG inhibit BetP to a different extent, (ii) betaine taken up by BetP is exported again *via* the various forms of MscCG to a different extent, and (iii) various forms of MscCG compromise the electrochemical Na^+ potential, the driving force of betaine uptake, to a different extent. Explanation (i) is very unlikely; consequently, we analyzed the second alternative using a previously developed pulse-chase technique for quantification of betaine influx and efflux [34]. We found enhanced betaine efflux in strain MscCG-Δ247-His (results not shown); because of inefficient betaine uptake, strain MscCG-Δ110-His could not be analyzed. To test the third hypothesis, we measured the membrane potential. For the analysis of betaine uptake upon osmotic shock, cells are first washed in hypoosmotic medium for depletion of solutes, before being exposed to hyperosmotic conditions for activating BetP. This procedure is not required for analyzing the driving force. Consequently we measured the membrane potential at three different conditions, (i) in washed cells without osmotic shock, (ii) in cells exposed to hyperosmotic conditions without prior downshock (control), and (iii) in cells after the usual cycle of hypo-osmotic washing and hyperosmotic shock (Table 3). All cells maintained a high electrical potential under basic conditions. This changed upon exposure to the washing cycle. The wild type kept a high potential, which was lower in MscCG-Δ247-His cells, and significantly reduced in cells harboring MscCG-Δ110-His. The relatively high standard deviation of the values for MscCG-Δ247-His cells is due to the fact that the membrane potential slightly increased during the measurement (15–45 min after osmotic shock). Taken together, the reason for the decreased betaine accumulation turned out to be a combination of models 2 (increased efflux) and 3 (decreased driving force), thus indicating the contribution of MscCG and its derivatives to the observed phenotype.

3.3. Glutamate excretion in *C. glutamicum* cells harboring truncated versions of MscCG

Glutamate export of the wild type, the deletion mutant, and the *mscCG* complementation strain was tested (Fig. 4A and Table 4). Glutamate excretion is shown as a result of penicillin addition; similar results were obtained using alternative methods to trigger glutamate export, e.g. biotin limitation or addition of Tween 60 [36–38] (results not shown). Deletion of *mscCG* led to a loss of about 70% of glutamate export, similar as reported previously [1,8]. Plasmid-borne expression of *mscCG* fully complemented glutamate excretion. Although the expression of individual constructs varied strongly, the efflux rate upon addition of penicillin did not vary strongly, as shown for *mscCG*-His and all truncation constructs in the absence and presence

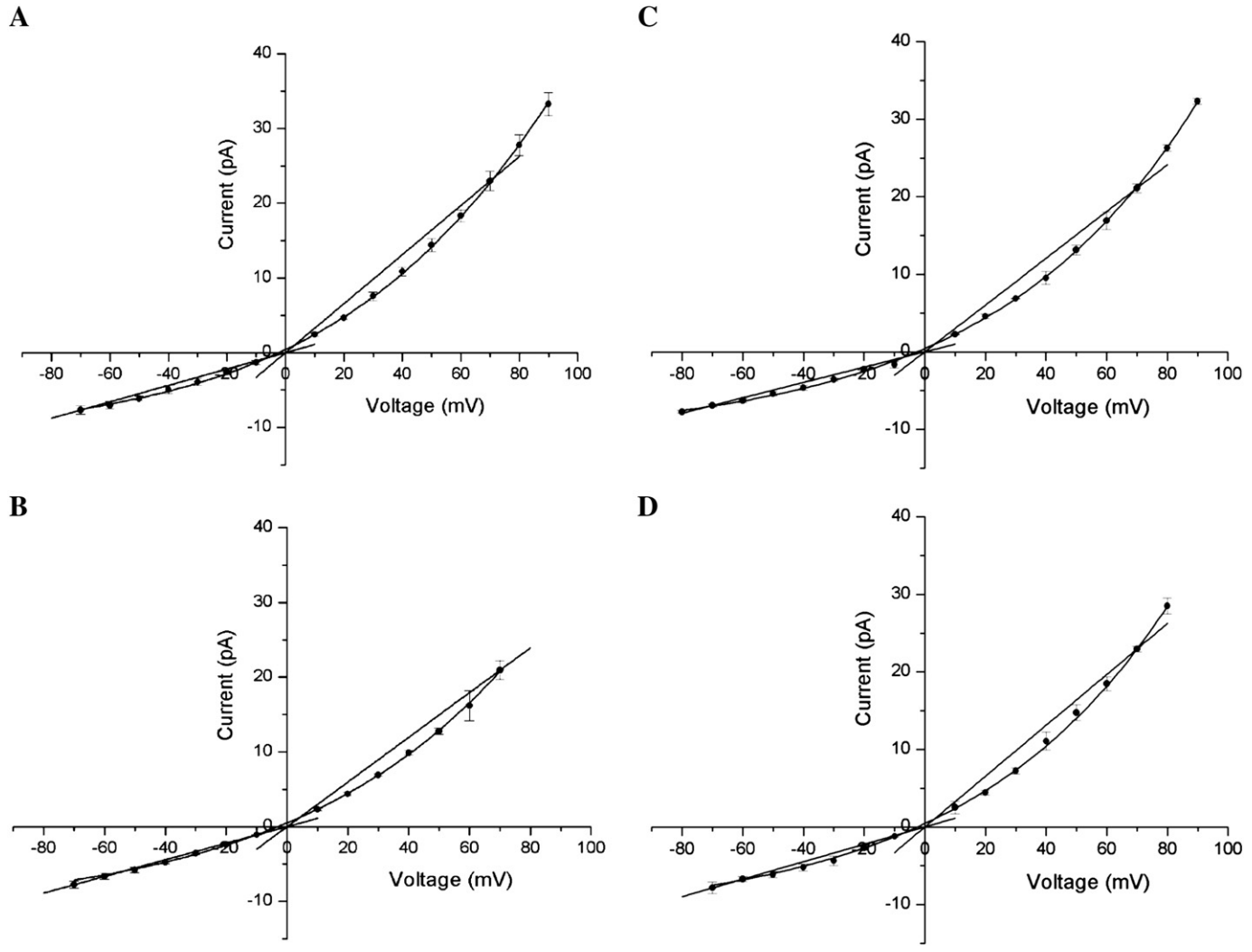

Fig. 3. Current/voltage relationship of MscCG in *E. coli* spheroplasts under asymmetrical conditions (pipette solution: 200 mM KCl, 40 mM $MgCl_2$, 5 mM HEPES; bath solution: 250 mM KCl, 90 mM $MgCl_2$, 5 mM HEPES). Straight lines are linear regressions in the voltage range of 0 to 70 mV (positive) and 0 to −70 mV (negative), crossing the origin and the current obtained at 70 mV and −70 mV, respectively. The slope of the linear regression results in the chord conductance. The following *mscCG* constructs were expressed in *E. coli* MJF612 (A) wild type *mscCG*, (B) *mscCG*-Δ110-His, (C) *mscCG*-Δ141-His, and (D) *mscCG*-Δ247-His.

of IPTG (Table 4, Fig. 1D). The recombinant strains behaved differently in the absence of added penicillin. Strain MscCG-Δ110-His excreted glutamate independently of any specific treatment, and low excretion was observed in the strain overexpressing the His-tagged version of MscCG (Fig. 4B and Table 4). Upon addition of penicillin, strain MscCG-Δ247-His and MscCG-Δ141-His resembled the wild type with respect to glutamate excretion (Table 4). Glutamate

Table 2
Electrophysiological characterization of MscCG, MscG truncation mutants, and fusion constructs with MscS, expressed in *E. coli* MJF612.

Construct expressed	Conductance (pS) at voltage polarity	
	Negative	Positive
mscCG	110	328
mscCG-Δ110[a]	111	299
mscCG-Δ141	99	302
mscCG-Δ247	112	328
mscS	87	1360
mscS-(C-MscCG)[b]		1310

The values for electrical conductance derived from I/V plots of the respective mutants at negative and positive voltage, respectively, are shown (see Fig. 3). The I/V plots for the MscS-fusion constructs are not shown, conductances were derived as in Fig. 3.

[a] This value was measured in the presence of 50 μM $GdCl_3$, added 15 min prior to the electrophysiological measurement (see text). The values are derived from I/V plots where corresponding standard deviation of each value is given.

[b] In the case of the MscS-(C-MscCG) construct, strong flickering in the negative voltage range occurred which prevented reliable calculation of conductance.

Table 3
Membrane potential of *C. glutamicum* strains harboring different truncated constructs of MscCG.

Conditions	I	II	III
Construct expressed	Membrane potential (mV)		
No (wild type)	185	199	196 ± 5
mscCG-Δ247-His	186	195	171 ± 8
mscCG-Δ110-His	182	178	138 ± 1

The indicated constructs were expressed in the *mscCG* deletion strain of *C. glutamicum*, except for the first line, where the wild type was used. For induction 25 μM IPTG was added. The membrane potential was determined under the following conditions: (I) incubation in buffer at 1.3 osmol/kg, no further treatment (uptake buffer, see Materials and methods section), (II) transfer to hyperosmotic conditions at 1.8 osmol/kg (hyperosmotic buffer, see Materials and methods section), and (III) cycle of hypoosmotic washing and hyperosmotic incubation (see Materials and methods section). The values listed for condition (III), which is most relevant because it represents the experimental conditions used in the glutamate efflux analysis, are means of at least three experiments.

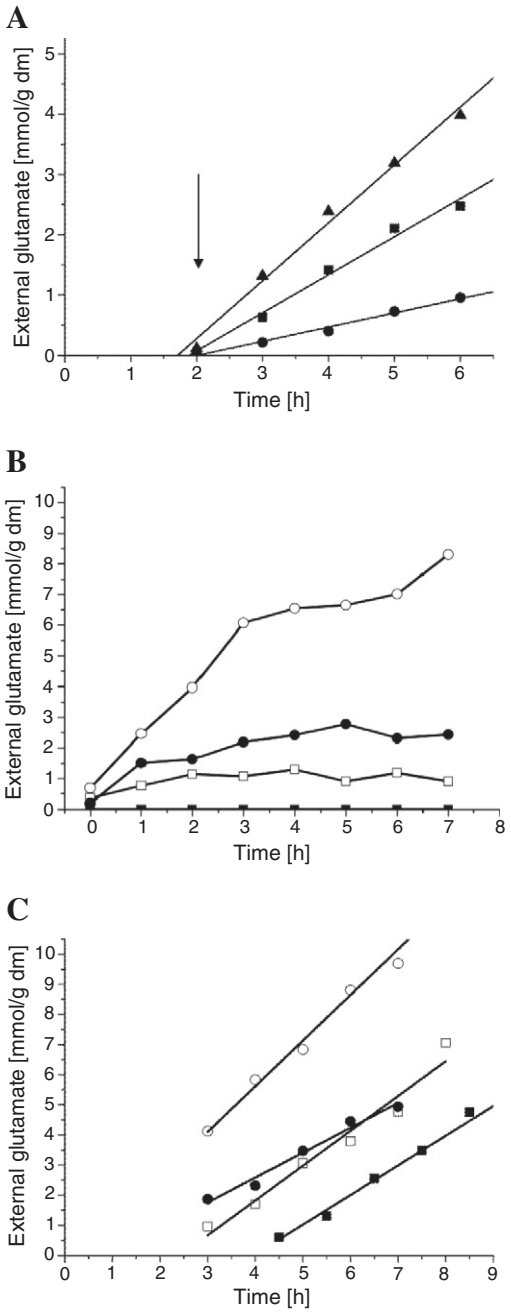

Fig. 4. Glutamate excretion upon addition of penicillin in *C. glutamicum* in dependence of the presence of *mscCG* and mutant forms of it. (A) Penicillin-triggered glutamate excretion in *C. glutamicum* wild type (squares), *mscCG* deletion mutant (circles) and complementation strain (triangles). (B) Glutamate excretion in the absence of penicillin by *C. glutamicum* wt (solid squares) and *mscCG* deletion strain expressing the following constructs: *mscCG*-His (open squares), *mscCG*-Δ110-His (solid circles), *mscCG*-His (A106V, GOF) (open circles). (C) Glutamate excretion of the same strains as in panel (B) upon addition of penicillin (3 h after start of the experiment). Panel (C) represents the same experiment and the same time scale as panel (B), the results of penicillin-triggered excretion are separated from panel (B) only for the sake of clarity. For expression, 25 μM IPTG was used. The values for the glutamate excretion rates are listed in Table 4. The time point when penicillin was added is indicated by an arrow.

excretion in strain MscCG-Δ110-His was not faster than that of the wild type, however, due to excretion already prior to penicillin addition, cells started at an increased level of external glutamate.

It may be argued that the values measured for the increase of external glutamate concentration do not correctly reflect excretion because of a possible concomitant glutamate uptake masking excretion activity to some extent. Consequently, we quantified glutamate uptake in separate experiments using cells treated identically to Fig. 4B. Glutamate uptake was below 2 $\mu mol \cdot g\ dm^{-1} \cdot min^{-1}$ in all strains tested and thus did not significantly interfere with our measurements (results not shown). It has previously been shown that glutamate uptake activity is down-regulated under glutamate excretion conditions [39].

3.4. Correlation of channel activity and glutamate excretion

These experiments are still not sufficient to unequivocally decide whether the channel domain of MscCG is responsible for glutamate export. As a further tool to study this we used *E. coli* MscS besides MscCG. The properties of MscS are known in detail and both gain-of-function (GOF) and loss-of-function (LOF) mutants were generated, in which particular amino acids involved in gating were altered [40–42]. Moreover, this approach offers an independent strategy to test the impact of the MscCG C-terminal domain on channel function when fused to the *E. coli* MscS protein. The constructs used for this analysis were tested for expression (Fig. 5).

We used a modeling approach to identify amino acid positions in MscCG resembling positions in MscS described to lead to LOF or GOF phenotypes. The sequence comparison of MscS and MscCG as well as structure modeling used is explained in detail in Fig. S2. We generated two GOF constructs (A106V and L109C), resulting in an increase in glutamate excretion compared to the wild type (Fig. 4C and Table 4). Notably, the A106V GOF mutant of MscCG effectively excreted glutamate already prior to the penicillin addition (Fig. 4B, expression in Fig. 1D), which had previously been demonstrated also for the GOF mutant MscCG A111V [1,6]. Whereas spontaneous glutamate excretion was only transient in the MscCG-Δ110-His strain, the GOF mutant was characterized by continuous export during 7 h (Fig. 4B). Construction of LOF mutants by structure modeling turned out to be difficult, because of the low similarity of TM segment 1 in MscCG and MscS. Finally, we succeeded in generating a double mutant MscCG Q112L,V115S, which, upon expression (Fig. 1D), showed low glutamate excretion in the presence of penicillin, similar to the value of the deletion mutant (Table 4). This LOF mutant of MscCG was proven in patch clamp measurements to be characterized by a significantly increased gating threshold (see below, Fig. 6). Interestingly, a truncation of the C-terminal 110 amino acids, which was shown above to lead to constitutive glutamate efflux activity of MscCG, was able to overcome the LOF phenotype and forced the LOF-type pore domain to effective glutamate excretion.

As an alternative approach, we expressed different *mscS* constructs in the *C. glutamicum mscCG* deletion strain. Besides MscS-His, we generated two LOF mutants, A51N/F68N and I37N/L86N [42], and two GOF mutants, L109S and A106V [40,41]. Expression of LOF mutants did not result in a growth phenotype, whereas GOF mutants affected growth even without added IPTG (results not shown). In Table 4, glutamate excretion by several of these mutant strains is listed. Surprisingly, penicillin addition triggered glutamate excretion in a strain expressing *mscS*-His to a level significantly exceeding the background of the deletion strain, although less effective than in *C. glutamicum* wild type harboring MscCG. Introduction of an LOF mutation (A51N/F68N) into the *mscS*-His construct reduced glutamate excretion to the level of the *mscCG* deletion strain.

We furthermore investigated a possible impact of the C-terminal domain of *C. glutamicum* MscCG on *E. coli* MscS. Unexpectedly, the fusion construct MscS-(C-MscCG)-His, i.e. a protein of the size of MscCG harboring the channel domain of MscS, was capable of effective glutamate excretion, nearly equaling that of MscCG (Table 4). Fusion of the truncated version of the MscCG C-terminal domain (Δ110), however, which leads to high and constitutive glutamate efflux in MscCG, did not increase efflux above the activity of MscS when fused to the wild type form of the MscCG C-terminal domain. Introduction of a LOF mutation (A51N/F86N) in the MscS channel of the MscS-(C-MscCG)-His

Table 4
Glutamate excretion rates in *C. glutamicum* strains harboring MscCG- and MscS-derived constructs triggered by addition of penicillin.

Strain	Expressed construct	Glutamate excretion rate (μmol g dm^{-1} min^{-1})			
		No IPTG		+ IPTG	
		No Penicillin	+ Penicillin	No penicillin	+ Penicillin
Wild type	No	0.0	16.6 ± 2.1		
mscCG deletion	No	0.0	3.4 ± 0.1		
	mscCG -His	0.0	19.1 ± 3.0	(16.5 ± 1.6)	19.2 ± 3.2
	mscCG-Δ110-His			(*15.2 ± 0.6*)	*15.0 ± 1.9*
	mscCG-Δ141-His	0.0	17.5 ± 0.9	0.0	18.6 ± 0.6
	mscCG-Δ247-His			0.0	19.0 ± 1.9
	mscCG-His (A106V, GOF)			20.3 ± 2.5	22.0 ± 3.0
	mscCG-His (Q112L,V115S, LOF)			0.0	3.7 ± 0.2
	mscCG-Δ110-His (Q112L, V115S, LOF)			(13.9 ± 1.1)	20.1 ± 0.4
	mscS-His			0.0	9.8 ± 0.7
	mscS-His (A51N, F68N, LOF)				5.8 ± 1.7
	mscS-(C-MscCG)-His			0.0	14.0 ± 0.8
	mscS-(C-MscCG)-His (A51N, F68N, LOF)				4.7 ± 1.2
	mscS-(C-MscCG-Δ110)-His			0.0	15.4 ± 0.8

For expression 25 μM IPTG was used except when indicated. For triggering glutamate excretion, 6 U/ml of penicillin was added. Values are listed with standard deviation. Glutamate excretion rates in the absence of penicillin were estimated based on the initial phase of excretion (see Fig. 3B). All results are means of at least three experiments. The value of 0.0 μmol·g dm^{-1}·min^{-1} reflects the absence of any external glutamate in the measurement. Underlined values indicate constructs for which high expression was observed, whereas values in italics represent data from constructs expressed at very low levels. Values in brackets indicate transient efflux activity during the first hours after addition of cultivation only (see Fig. 4B and text).

construct inactivated glutamate excretion proving also in the case of the *E. coli* MscS that glutamate export by the MscS-(C-MscCG)-His fusion is specific. As a control, we analyzed glutamate efflux in *C. glutamicum* cells expressing both *mscS* and *mscS*-(C-MscCG) constructs without a His-tag, and found values of excretion closely similar to those of the His-tagged versions (results not shown).

3.5. Patch-clamp characterization of MscCG and MscS derivatives

Finally we analyzed the electrophysiological properties of proteins used in these experiments. As shown before, truncated versions of MscCG did not differ in their conductance from the wild type protein (Table 2). The same was true for MscS compared with MscS-(C-MscCG). In spite of increasing glutamate excretion, fusion of the C-terminal domain of MscCG did not alter the conductance of MscS (Table 2, Fig. S3). Since we realized basic differences in the gating behavior of the two MscS-type proteins used in this study, MscS and MscCG, we analyzed the threshold of channel opening of the constructs in an appropriate *E. coli* strain (MFJ431, lacking MscS and MscK but not MscL) where it can be directly compared to the well-studied MscL channel (Fig. 6). The results clearly indicate that the extent of hypo-osmotic stress required to open MscCG is lower than that necessary for MscS gating. Besides not changing its conductance, fusion of the C-terminal domain of MscCG to MscS does also not significantly alter its threshold for channel opening, as proven by a detailed gating analysis (Fig. S4). Very interestingly, truncation of MscCG to the size of MscS (MscCG-Δ247) leads to an increase in the threshold ratio to values higher than that measured for MscS. As already mentioned above, the introduction of a Q112L,V115S amino acid replacement leading to a LOF phenotype is reflected by a significantly increased gating threshold (Fig. 6).

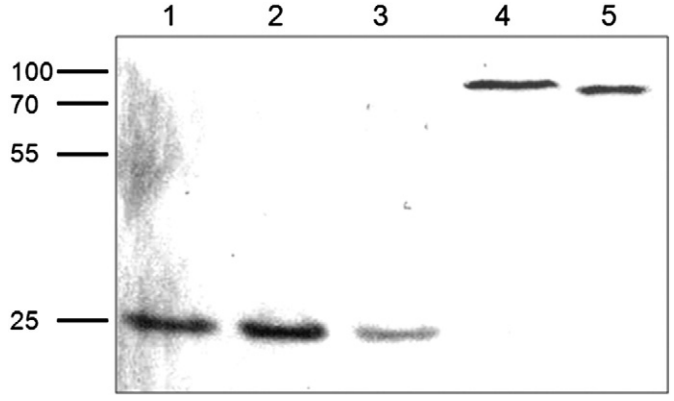

Fig. 5. Western blot analysis of *mscS* and *mscCG* constructs expressed in *C. glutamicum* Δ*mscCG*. Experimental conditions as described in Fig. 1D. 25 μg of the following proteins was applied: MscS-His (1), MscS-His (A51N, F68N) (LOF) (2), MscS-His (A106V) (GOF) (3), MscS-(C-MscCG)-His (4), and MscS-(C-MscCG)-His (A51N, F86N) (LOF) (5).

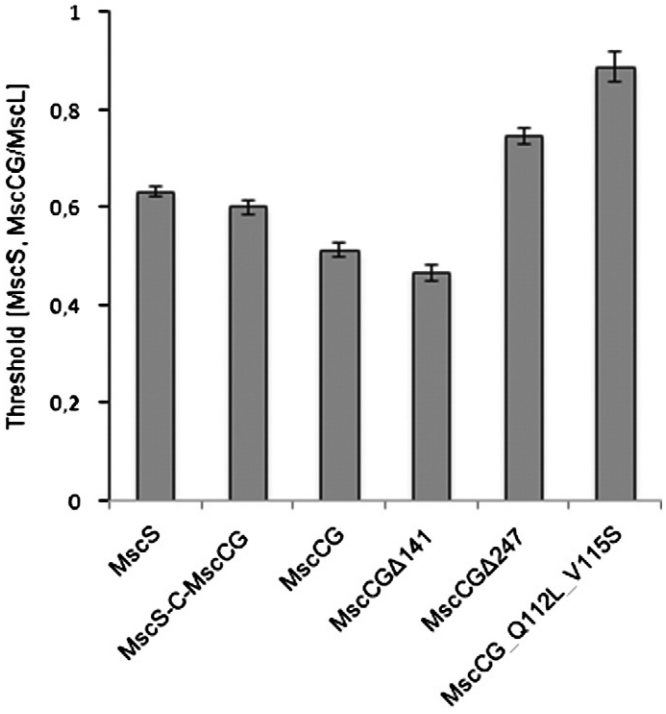

Fig. 6. Threshold ratio of various MscS and MscCG proteins and fusion constructs in *E. coli* MJF431. In the figure, the threshold ratio of all tested constructs in relation to MscL is given. Thresholds for gating were determined by patch-clamp measurements (mean ± SE, n ≥ 5).

4. Discussion

In this work, we addressed functional and/or regulatory properties of the unique C-terminal domain of MscCG and the direct assignment of channel function to glutamate efflux. For this purpose, we generated various recombinant forms of MscCG from *C. glutamicum* and MscS from *E. coli*, as well as fusion constructs of the MscCG C-terminal domain with the MscS channel. This led to a number of important and partially unexpected results. Heterologous expression of MscS in *C. glutamicum* devoid of MscCG, upon penicillin addition, led to glutamate efflux. Introduction of a LOF mutation in MscCG, which, to our knowledge is the first LOF mutant of this channel, abolished excretion proving its dependence on a functional channel domain. Correspondingly, this mutant showed an increased threshold of gating in patch clamp measurements. Its relative threshold ratio compared to MscL [25] is 0.89 indicating that this mutant requires more pressure for activation than MscL. The increased threshold ratio compares favorably with the decrease in the glutamate excretion ratio observed in this mutant (Table 4). Similarly, an engineered MscS LOF mutant lost its capability to excrete glutamate. The introduction of a GOF mutation in MscCG resulted in glutamate excretion in the absence of the penicillin trigger. The fact that the rate of glutamate excretion upon penicillin addition was not significantly increased in this GOF mutant compared to the wild type may be due to a partially compromised physiology of these strains, which is directly reflected in a severe growth phenotype. It should be pointed out that some of the mutations previously identified in *NCgl1221* from *C. glutamicum* ATCC13869 leading to increased glutamate efflux, e.g. A100T and A111V, most probably also represent GOF mutants, as has been mentioned by the authors [1].

Some aspects of these results are of particular interest. Beyond the finding that deletion and complementation of *mscCG* leads to a decrease and restoration, respectively, of penicillin triggered glutamate excretion in *C. glutamicum*, as shown previously [1], the assignment of amino acid flux to the function of the channel part by exploring LOF and GOF mutants of both MscS and MscCG strongly argues for glutamate, during triggered glutamate excretion, passing through the channel of MscCG. It is important to note the functional equivalence of *E. coli* and *C. glutamicum* MS channels. MscS is not only able to mediate glutamate excretion in *C. glutamicum*, albeit to a reduced extent, but glutamate efflux is surprisingly also triggered by penicillin, as previously only known for *C. glutamicum*. This is of core interest since the mechanism of triggering glutamate excretion in *C. glutamicum* by various stimuli is still far from being understood [36–38]. Notably, the cell wall of *C. glutamicum* is very different from that of *E. coli*, which is also reflected by differences in the action of penicillin [43]. Our results point towards a rather unspecific explanation for the penicillin-dependent trigger mechanism probably based on changes in general properties of the cell wall.

We used fusion constructs to investigate the impact of the MscCG C-terminal domain. Fusion of this domain to MscS results in a protein of the size of MscCG harboring the MscS channel. MscS expressed in *C. glutamicum* responded to penicillin treatment with low level glutamate excretion, but excretion was increased when the MscCG C-terminal domain was hooked up to the MscS channel. This argues for a regulatory role of the C-terminal peptide on the channel domain, even when originating from a heterologous source. Notably, sequence analysis shows a rather distant relationship of the MscCG and MscS channel (18% identical and 43% similar amino acids in the channel domains), which does not prevent MscS from being regulated by the MscCG C-terminal domain similar to MscCG.

The function of the C-terminal domain was studied using truncated versions, i. e. MscCG-Δ110-His, missing the periplasmic hydrophilic stretch of amino acids, MscCG-Δ141-His, lacking in addition the fourth transmembrane segment, and MscCG-Δ247-His, being truncated to exactly the size of *E. coli* MscS. The presence of MscCG-Δ110-His led to spontaneous glutamate excretion. This is in line with previous results obtained in a closely related species [1], where deletion of the terminal part of the C-terminal domain of NCgl1221 in *C. glutamicum* ATCC 13869 downstream valine at position 419 also resulted in constitutive glutamate efflux. MscCG-Δ247-His and MscCG-Δ141-His led to inducible glutamate excretion upon addition of penicillin with rates similar to those of the wild type. The impact of the C-terminal domain, however, can be recognized by the fact that high level expression of MscCG with the full length C-terminal domain leads to spontaneous glutamate excretion, whereas similar expression of *mscCG*-Δ141-His and *mscCG*-Δ247-His did not (Table 4).

These results matched the energetic situation. Cells harboring these constructs had normal values of the membrane potential when not stressed. This situation changed upon exposure to osmotic shock, and, in particular, the MscCG-Δ110 strain was compromised in maintaining a high electrical potential. This is obviously not a direct reaction to osmotic stress but a long term functional change of this protein. A mechanosensitive channel, when opening to equilibrate osmotic gradients, immediately closes again after equilibrium is reached. The MscCG constructs, after exposure to osmotic stress, seem to remain partially open for indefinite time.

In patch clamp experiments the conductance of the constructs was unaltered, indicating an unchanged pore size. This was also true for the MscS-(C-MscCG) fusion construct resembling MscS in its conductance, and thus argues for the C-terminal domain of MscG interacting with the channel in gating but not changing its pore structure. This is in line with a further interesting observation. When we compared the threshold of MscS and MscCG for channel opening, we found that MscCG needs less membrane tension for gating. This, however, was changed to values resembling or even exceeding those of MscS when the C-terminal domain of MscCG was removed resulting in a protein of the size of MscS.

The different expression levels of individual constructs did not significantly change their efflux behavior in the presence of penicillin, as shown, for example, by comparing the values for MscCG-His and MscCG-Δ141-His in the absence and presence of IPTG (Fig. 1D, Table 4). For so far unknown reasons, it seems that a maximum value of the rate of glutamate efflux exists, which cannot be exceeded even upon massive overexpression and introduction of a GOF mutation, respectively (Table 4).

Inhibition of glutamate efflux could be achieved by modifying the channel in either MscS or MscCG (LOF mutants). Vice versa, glutamate efflux, even in the absence of the penicillin trigger, may result from either channel mutations (GOF mutants of MscCG), the additional presence of the MscCG C-terminal domain (MscS-(C-MscCG), or from changes in this domain (MscCG-Δ110-His). The electrophysiological properties of the truncation mutants again argue for the observed differences being not due to changes in the channel conformation (pore size), but rather to a changed gating (open probability). Of particular interest is the result of the fusion construct combining an MscCG LOF mutation with the Δ110-His truncated C-terminal domain (MscCG-Δ110-His (Q112L, V115S)). The strong functional impact of the truncated domain can be recognized by the fact that in this recombinant form, the LOF phenotype is completely overcome by the strong tendency of Δ110 truncated constructs to excrete glutamate (Table 4).

Mechanistic explanations for a changed open probability in GOF or LOF mutants of MscS have been put forward [40,44]. Most probably, this is also true for MscCG, but the current lack of structural information prevents a mechanistic interpretation of the action of the C-terminal domain on MscCG function, discriminating MscCG from other MscS-like proteins. We suggest that this domain structurally interferes with gating of the channel in changing its open probability and its function in glutamate efflux. The surprising observation of the MscCG C-terminal domain forcing *E. coli* MscS to increased glutamate efflux argues for a general mechanism by which this domain may affect MscS-like proteins. A mechanistic description of MS channels of the MscCG type should thus include a functional model for both the channel and the C-terminal domain, and should also provide

an idea for the penicillin trigger leading to glutamate excretion. Our results indicate that excretion is mainly a matter of gating properties of the channel. We speculate that the 4th TM segment of MscCG interacts with the large cytoplasmic domain of MscS-type channels leading to conformational changes which may modulate the flow of solutes through the channel.

Taken together, an increased tendency to trigger glutamate excretion under particular conditions may be based on the construction of the channel, as indicated by the comparison of *E. coli* MscS and *C. glutamicum* MscCG-Δ247-His, which share the same size but differ in their efficiency of excretion. Glutamate excretion may also be caused by a specific function of the C-terminal domain of MscCG, as indicated by fusing it to MscS. Moreover, the strong impact of a modified version of this channel (Δ110) on the functional properties of MscCG but not MscS, demonstrates, on the one hand, the mechanistic significance of interaction. On the other hand, it also indicates that this interaction may, to some extent, be structurally specific, although the full length C-terminal domain of MscCG is in fact able to trigger glutamate excretion in the wild type form of MscS. Surprisingly, the penicillin trigger seems to work in both cases, irrespective whether the channel pore domain originates from MscS or MscCG, and irrespective whether a C-terminal domain is present or not. The different effectiveness of penicillin, however, being dependent on the type of channel used, argues for a direct impact of this trigger on the gating process of the channels.

Acknowledgements

We would like to thank Lothar Eggeling (Research Center Jülich) for the valuable help in topology determination, Christine Ziegler, Caroline Koshy and Katrin Rohde (Max-Planck-Institute for Biophysics, Frankfurt) for their help in designing constructs of MscCG and for their helpful interaction and Paul R. Rohde (Victor Chang Cardiac Research Institute) for his technical assistance. We are grateful to Michelle Edwards and Ian Booth (University of Aberdeen, Scotland) for providing *E. coli* strains MJF612, MFJ465, and MFJ431. We acknowledge the National Health and Medical Research Council of Australia, the Yamada Science Foundation and Ajinomoto Co. (Japan) for the financial support and Y. Hara (Ajinomoto Co.) for valuable cooperation.

Appendix A. Supplementary data

Supplementary data to this article can be found online at http://dx.doi.org/10.1016/j.bbamem.2013.01.001.

References

[1] J. Nakamura, S. Hirano, H. Ito, M. Wachi, Mutations of the *Corynebacterium glutamicum* NCgl1221 gene, encoding a mechanosensitive channel homolog, induce L-glutamic acid production, Appl. Environ. Microbiol. 73 (2007) 4491–4498.
[2] L. Eggeling, H. Sahm, New ubiquitous translocators: amino acid export by *Corynebacterium glutamicum* and *Escherichia coli*, Arch. Microbiol. 180 (2003) 155–160.
[3] R. Krämer, Secretion of amino acids by bacteria: physiology and mechanism, FEMS Microbiol. Rev. 13 (1994) 75–94.
[4] K. Marin, R. Krämer, Amino acid transport systems in biotechnologically relevant bacteria, in: V.F. Wendisch (Ed.), Microbiol Monogr, Springer, Heidelberg, 2007, pp. 290–325.
[5] M.D. Island, R.J. Kadner, Interplay between the membrane-associated UhpB and UhpC regulatory proteins, J. Bacteriol. 175 (1993) 5028–5034.
[6] Y. Nakayama, K. Yoshimura, H. Iida, A gain-of-function mutation in gating of *Corynebacterium glutamicum* NCgl1221 causes constitutive glutamate secretion, Appl. Environ. Microbiol. 78 (2012) 5432–5434.
[7] K. Hashimoto, J. Murata, T. Konishi, I. Yabe, T. Nakamatsu, H. Kawasaki, Glutamate is excreted across the cytoplasmic membrane through the NCgl1221 channel of *Corynebacterium glutamicum* by passive diffusion, Biosci. Biotechnol. Biochem. 76 (2012) 1422–1424.
[8] K. Borngen, A.R. Battle, N. Moker, S. Morbach, K. Marin, B. Martinac, R. Kramer, The properties and contribution of the *Corynebacterium glutamicum* MscS variant to fine-tuning of osmotic adaptation, Biochim. Biophys. Acta 1798 (2010) 2141–2149.
[9] D. Nottebrock, U. Meyer, R. Krämer, S. Morbach, Molecular and biochemical characterization of mechanosensitive channels in *Corynebacterium glutamicum*, FEMS Microbiol. Lett. 218 (2003) 305–309.
[10] B. Martinac, Mechanosensitive channels in prokaryotes, Cell. Physiol. Biochem. 11 (2001) 61–76.
[11] S.G. Grant, J. Jessee, F.R. Bloom, D. Hanahan, Differential plasmid rescue from transgenic mouse DNAs into *Escherichia coli* methylation–restriction mutants, Proc. Natl. Acad. Sci. U. S. A. 87 (1990) 4645–4649.
[12] R. Rübenhagen, H. Rönsch, H. Jung, R. Krämer, S. Morbach, Osmosensor and osmoregulator properties of the betaine carrier BetP from *Corynebacterium glutamicum* in proteoliposomes, J. Biol. Chem. 275 (2000) 735–741.
[13] M. Jakoby, R. Krämer, A. Burkovski, Nitrogen regulation in *Corynebacterium glutamicum*: isolation of genes involved and biochemical characterization of corresponding proteins, FEMS Microbiol. Lett. 173 (1999) 303–310.
[14] J. Yon, M. Fried, Precise gene fusion by PCR, Nucleic Acids Res. 17 (1989) 4895.
[15] M. Seidel, L.J. Alderwick, H. Sahm, G.S. Besra, L. Eggeling, Topology and mutational analysis of the single Emb arabinofuranosyltransferase of *Corynebacterium glutamicum* as a model of Emb proteins of *Mycobacterium* tuberculosis, Glycobiology 17 (2007) 210–219.
[16] K. Arnold, L. Bordoli, J. Kopp, T. Schwede, The SWISS-MODEL workspace: a web-based environment for protein structure homology modelling, Bioinformatics 22 (2006) 195–201.
[17] R.B. Bass, P. Strop, M. Barclay, D.C. Rees, Crystal structure of *Escherichia coli* MscS, a voltage-modulated and mechanosensitive channel, Science 298 (2002) 1582–1587.
[18] V. Belyy, A. Anishkin, K. Kamaraju, N. Liu, S. Sukharev, The tension-transmitting 'clutch' in the mechanosensitive channel MscS, Nat. Struct. Mol. Biol. 17 (2010) 451–458.
[19] A.M. Waterhouse, J.B. Procter, D.M. Martin, M. Clamp, G.J. Barton, Jalview version 2—a multiple sequence alignment editor and analysis workbench, Bioinformatics 25 (2009) 1189–1191.
[20] C. Notredame, D.G. Higgins, J. Heringa, T-Coffee: a novel method for fast and accurate multiple sequence alignment, J. Mol. Biol. 302 (2000) 205–217.
[21] N. Eswar, B. Webb, M.A. Marti-Renom, M.S. Madhusudhan, D. Eramian, M.Y. Shen, U. Pieper, A. Sali, Comparative protein structure modeling using MODELLER, Curr. Protoc. Protein Sci. (2007), (Chapter 2, Unit 2 9).
[22] U. Schumann, M.D. Edwards, T. Rasmussen, W. Bartlett, P. van West, I.R. Booth, YbdG in *Escherichia coli* is a threshold-setting mechanosensitive channel with MscM activity, Proc. Natl. Acad. Sci. 107 (2010) 12664–12669.
[23] N. Levina, S. Totemeyer, N.R. Stokes, P. Louis, M.A. Jones, I.R. Booth, Protection of *Escherichia coli* cells against extreme turgor by activation of MscS and MscL mechanosensitive channels: identification of genes required for MscS activity, EMBO J. 18 (1999) 1730–1737.
[24] B. Martinac, M. Buechner, A.H. Delcour, J. Adler, C. Kung, Pressure-sensitive ion channel in *Escherichia coli*, Proc. Natl. Acad. Sci. U. S. A. 84 (1987) 2297–2301.
[25] I. Iscla, G. Levin, R. Wray, R. Reynolds, P. Blount, Defining the physical gate of a mechanosensitive channel, MscL, by engineering metal-binding sites, Biophys. J. 87 (2004) 3172–3180.
[26] E. Brickman, J. Beckwith, Analysis of the regulation of *Escherichia coli* alkaline phosphatase synthesis using deletions and phi80 transducing phages, J. Mol. Biol. 96 (1975) 307–316.
[27] J.H. Miller, A short course in bacterial genetics, A laboratory Manual and Handbook for *Escherichia coli* and Related Bacteria, Cold Spring Harbour Laboratory Press, New York, 1992.
[28] B. Landfald, A.R. Strom, Choline–glycine betaine pathway confers a high level of osmotic tolerance in *Escherichia coli*, J. Bacteriol. 165 (1986) 849–855.
[29] M. Gutmann, C. Hoischen, R. Krämer, Carrier-mediated glutamate secretion by *Corynebacterium glutamicum* under biotin limitation, Biochim. Biophys. Acta 1112 (1992) 115–123.
[30] R. Krämer, C. Lambert, Uptake of glutamate in *Corynebacterium glutamicum*. 2. Evidence for a primary active transport system, Eur. J. Biochem. 194 (1990) 937–944.
[31] H. Rottenberg, Non-equilibrium thermodynamics of energy conversion in bioenergetics, Biochim. Biophys. Acta 549 (1979) 225–253.
[32] M.M. Bradford, A rapid and sensitive method for the quantitation of microgram quantities of protein utilizing the principle of protein-dye binding, Anal. Biochem. 72 (1976) 248–254.
[33] W. Yao, X. Deng, M. Liu, P. Zheng, Z. Sun, Y. Zhang, Expression and localization of the *Corynebacterium glutamicum* NCgl1221 protein encoding an L-glutamic acid exporter, Microbiol. Res. 164 (2009) 680–687.
[34] J. Botzenhardt, S. Morbach, R. Krämer, Activity regulation of the betaine transporter BetP of *Corynebacterium glutamicum* in response to osmotic compensation, Biochim. Biophys. Acta 1667 (2004) 229–240.
[35] H. Peter, A. Burkovski, R. Krämer, Isolation, characterization, and expression of the *Corynebacterium glutamicum* betP gene, encoding the transport system for the compatible solute glycine betaine, J. Bacteriol. 178 (1996) 5229–5234.
[36] T.D. Nunheimer, J. Birnbaum, E.D. Ihnen, A.L. Demain, Product inhibition of the fermentative formation of glutamic acid, Appl. Microbiol. 20 (1970) 215–217.
[37] I. Shiio, S.I. Otsuka, M. Takahashi, Effect of biotin on the bacterial formation of glutamic acid. I. Glutamate formation and cellular permeability of amino acids, J. Biochem. 51 (1962) 56–62.
[38] K. Takinami, H. Yoshii, H. Tsuri, H. Okada, Biochemical effects of fatty acid and its derivatives on L-glutamic acid fermentation. Part III. Biotin–Tween 60 relationship in the accumulation of L-glutamic acid and the growth of *Brevibacterium lactofermentum*, Agric. Biol. Chem. 29 (1965) 351–359.
[39] R. Krämer, C. Hoischen, Futile cycling caused by the simultaneous presence of separate transport systems for uptake and secretion of amino acids in *Corynebacterium*

glutamicum, in: H. Westerhoff (Ed.), Biothermokinetics, Intercept Publ., Amsterdam, 1994, pp. 19–26.
[40] S. Miller, W. Bartlett, S. Chandrasekaran, S. Simpson, M. Edwards, I.R. Booth, Domain organization of the MscS mechanosensitive channel of *Escherichia coli*, EMBO J. 22 (2003) 36–46.
[41] M.D. Edwards, Y. Li, S. Kim, S. Miller, W. Bartlett, S. Black, S. Dennison, I. Iscla, P. Blount, J.U. Bowie, I.R. Booth, Pivotal role of the glycine-rich TM3 helix in gating the MscS mechanosensitive channel, Nat. Struct. Mol. Biol. 12 (2005) 113–119.
[42] T. Nomura, M. Sokabe, K. Yoshimura, Lipid-protein interaction of the MscS mechanosensitive channel examined by scanning mutagenesis, Biophys. J. 91 (2006) 2874–2881.
[43] V. Puech, M. Chami, A. Lemassu, M.A. Laneelle, B. Schiffler, P. Gounon, N. Bayan, R. Benz, M. Daffe, Structure of the cell envelope of corynebacteria: importance of the non-covalently bound lipids in the formation of the cell wall permeability barrier and fracture plane, Microbiology 147 (2001) 1365–1382.
[44] S. Sukharev, B. Akitake, A. Anishkin, The bacterial mechanosensitive channel MscS: emerging principles of gating and modulation, Curr. Top. Membr. 58 (2007) 235–267.